



Technical note

Design and construction of geocell foundation to support the embankment on settled red mud

T.G. Sitharam¹, A. Hegde*

Department of Civil Engineering, Indian Institute of Science, Bangalore 560012, India

ARTICLE INFO

Article history:

Received 15 March 2013
 Received in revised form
 24 July 2013
 Accepted 3 August 2013
 Available online 24 August 2013

Keywords:

Geocells
 Embankment
 Red mud
 Bearing capacity
 Strip footing
 Model tests

ABSTRACT

This paper presents the case history of the construction of a 3 m high embankment on the geocell foundation over the soft settled red mud. Red mud is a waste product from the Bayer process of Aluminum industry. Geotechnical problems of the site, the design of the geocell foundation based on experimental investigation and the construction sequences of the geocell foundations in the field are discussed in the paper. Based on the experimental studies, an analytical model was also developed to estimate the load carrying capacity of the soft clay bed reinforced with geocell and combination of geocell and geogrid. The results of the experimental and analytical studies revealed that the use of combination of geocell and the geogrid is always beneficial than using the geocell alone. Hence, the combination of geocell and geogrid was recommended to stabilize the embankment base. The reported embankment is located in Lanjigharh (Orissa) in India. Construction of the embankment on the geocell foundation has already been completed. The constructed embankment has already sustained two monsoon rains without any cracks and seepage.

© 2013 Elsevier Ltd. All rights reserved.

1. Introduction

Embankments are an integral part of roads, railways, canals and earth dams and other storage utilities. Often embankments are constructed over soft soils. Short term stability is the major governing criterion in the design of embankments since the foundation soil gains the strength with the time due to consolidation. Generally, ground improvement techniques such as vibro stone columns are used to strengthen the embankment bases in soft soils. However, the more recent trend is to use the geosynthetic reinforcements (eg. geotextiles, geogrids) to enhance the stability of the embankments. Studies conducted by many researchers have confirmed the suitability of geosynthetic reinforcements in such applications (Basudhar et al., 2008; Bergado and Teerawattanasuk, 2008; Chen et al., 2008; Ghazavi and Lavasan, 2008; Li and Rowe, 2008; Rowe and Taechakumthorn, 2008; Abusharar et al., 2009; Huang and Han, 2009; Magnani et al., 2009; Subaida et al., 2009; Zheng et al., 2009; Indraratna et al., 2010; Jones et al., 2010; Karstunen and Yin, 2010; Wang et al., 2011; Fan and Hsieh, 2011;

Rowe and Taechakumthorn, 2011; Demir et al., 2013; Bai et al., 2013). Generally, geosynthetic reinforcements are provided to enhance the tension resistance of the soil. Often these methods are coupled with the wick drains and PVDs (Sharma and Bolton, 2001; Lorenzo et al., 2004; Chu et al., 2006; Rowe and Taechakumthorn, 2008; Sinha et al., 2009; Saowapakpiboon et al., 2010; Karunaratne, 2011; Indraratna et al., 2012). Wick drains expedite the consolidation process and increases the shear strength of the soil. Geocells are three dimensional expandable panels made up of high density polymers. Many researchers have reported the beneficial effects of geocells (Dash et al., 2001a; Sitharam and Sireesh, 2005; Zhou and Wen, 2008; Madhavi Latha and Somwanshi, 2009; Sireesh et al., 2009; Moghaddas Tafreshi and Dawson, 2010; Pokharel et al., 2010; Lambert et al., 2011; Moghaddas Tafreshi and Dawson, 2012; Tavaloli Mehrjardi et al., 2012; Yang et al., 2012; Thakur et al., 2012; Mehdipour et al., 2013; Leshchinsky and Ling, 2013).

Very limited information is available in the literature about the geocell supported embankments. Jenner et al. (1988) proposed a methodology based on slip line theory to design the geocell foundation system for stabilizing the base of an embankment. Krishnaswamy et al. (2000) presented the beneficial effect of geocell reinforcement in stabilizing the base of an embankment through the laboratory 1-g model tests. Madhavi Latha (2000) proposed FEM based approach to design of the geocell reinforced

* Corresponding author. Tel.: +91 8277381341; fax: +91 80 23600404/23602261.
 E-mail addresses: sitharam@civil.iisc.ernet.in (T.G. Sitharam), amarnathhegde@gmail.com (A. Hegde).

¹ Tel.: +91 80 23602261/22932919; fax: +91 80 23600404/23602261.

embankment based on the equivalent composite approach. In this model, induced apparent cohesion in the geocell-soil composite was related to the increment in the confining pressure on the soil due to the provision of the geocell reinforcement. Further, based on the equivalent composite approach, Madhavi Latha et al. (2006) proposed the slope stability based design approach to design the geocell supported embankment. This method uses a general-purpose slope stability program. Zhang et al. (2010) proposed analytical method to find the bearing capacity of the geocell reinforced clay bed supporting an embankment. In this method, the increase in bearing capacity was attributed to the vertical stress dispersion effect and the membrane effect.

The majority of the previous research is oriented towards developing the design procedures for the geocell supported embankments and highlighting the beneficial effects of geocells through experimental studies. In spite of the recent developments, the use of geocells to stabilize the embankment base has not gained enough popularity due to non-availability of proven case histories. Also in the past, use of geocells in stabilizing the embankments is restricted only to road and rail embankments in the transportation sectors. Cowland and Wong (1993) reported a case history of a 10 m high road embankment construction on the geocell foundation in soft clay deposits in Hong Kong. Geocell technique was coupled with wick drains in the reported work. The present study brings out the innovative field application of geocells in stabilizing the embankment base in Aluminum mine tailing i.e soft settled red mud. The reported work is first of its kind in India. Geotechnical problems of the site, the design of the geocell foundation based on experimental investigation and construction sequences of the geocell foundation at the field are discussed in the paper. Based on the experimental studies, an analytical method was also developed to estimate the load carrying capacity of the soft clay bed reinforced with geocell and combination of geocell and geogrid.

2. Site description and background

The reported site is located in Lanjigarh, Orissa in India. The embankment was part of a red mud pond, used to store the red mud. Red mud is a waste product from the Bayer process of Alumina recovery. It contains solid and metallic oxide-bearing impurities, causing serious disposal problems. The red mud is a poor construction material which comes out in a semi-liquid state with 65%–70% solids. The existing pond was facing severe capacity constraint. Height of the embankment surrounding the red mud pond had to be raised in order to increase the capacity. Due to the area constraint, upstream method of embankment rising was adopted. This has led to the situation of constructing the new embankment of 680 m long, 20 m wide and 3 m in height on the settled red mud itself. Fig. 1 shows the location and typical cross section of the embankment.

3. Subsoil profile

Three bore holes were drilled in the vicinity. At the proposed location, 12 m thick settled red mud was observed. The SPT-N value of 9 was observed at the depth of 2 m. Beyond 4 m, over consolidated stiff red mud was observed with SPT-N value more than 14. Stagnated water at many places had made the red mud very soft. The red mud was classified as inorganic clay with low to medium plasticity (CL) as per Unified Soil Classification System (USCS). The bulk density and the water content of the red mud was 22 kN/m³ and 20% respectively. Fig. 2 shows the idealized soil profile of the area with the mention of different properties of the red mud.

4. Laboratory experiments

The primary aim of the laboratory study was to ascertain the suitability of the geocell foundation in soft clays. To obtain the realistic comparison with the field, the clay bed was prepared with undrained cohesion of 10 kPa. Neoweb geocells with effective pocket diameter 0.21 m and yield tensile strength 20 kN/m were used as the reinforcements. A biaxial geogrid (SS-20) with ultimate tensile strength 20 kN/m was also used in the experimental investigation. The staged construction of the embankment in plain strain condition was simulated by applying the incremental load on the strip footing placed along the width of the tank. The strip footing used was 20 mm thick, 150 mm wide and 750 mm long and was made up of steel. Three numbers of stress controlled plate load tests were conducted viz. unreinforced, geocell reinforced and geocell reinforced with additional basal geogrid.

4.1. Experimental setup

A cast iron test tank of 1800 mm long, 800 mm wide and 1200 mm in height was used in the experimental investigation. The tank was connected to the loading frame and which was internally connected to manually operated hydraulic jack. A 20 mm thick steel plate with width 150 mm and length 750 mm was used as the footing. The bottom of the footing was made rough by coating a thin layer of sand with epoxy glue. The load was applied on the footing through the hydraulic jack. A pre-calibrated proving ring was placed between the footing and hydraulic jack to measure the applied load. A ball bearing arrangement was used to prevent the eccentric application of the load. Fig. 3 represent the schematic view of the test setup.

4.2. Materials used

Natural silty clay with specific gravity 2.66 was used to prepare the foundation bed. The liquid limit and the plastic limit of the clay were 40% and 19% respectively. As per Unified Soil Classification System, clay was classified as clay with low to medium plasticity (CL). The maximum dry density and the optimum moisture content of the soil in the Standard Proctor test were 18.2 kN/m³ and 13.2% respectively. Dry sand was used to fill the geocell pockets. Sand was having specific gravity 2.64, effective particle size (D_{10}) 0.26 mm, coefficient of uniformity (C_u) 3.08, coefficient of curvature (C_c) 1.05, maximum void ratio (e_{max}) 0.81, minimum void ratio (e_{min}) 0.51 and angle of internal friction (ϕ) 40°. As per Unified Soil Classification System, the sand was classified as poorly graded sand with symbol SP. Grain size distribution of both sand and clay are shown in Fig. 4. The properties of the geocell and geogrid as provided by the manufacturer, PRS Mediterranean Ltd. Israel, are listed in Table 1.

4.3. Preparation of clay bed

Firstly, the dry clay was powdered and mixed with the pre-determined amount of water. The moist soil was placed in the airtight container for 3–4 days for allowing uniform distribution of moisture within the sample before kneading it again. The sides of the tank were covered with Polythene sheets to avoid the side friction. Foundation bed of 900 mm thick was prepared by compacting the soil uniformly in layers of 25 mm each. The fall cone apparatus was used to measure the undrained cohesion values at different locations during different stages of the bed preparation. The fall cone apparatus provides rapid and accurate measurement of undrained shear strength. By carefully controlling the compaction effort and the water content of the test bed, an undrained cohesion value of 10 kPa was maintained in all the tests.

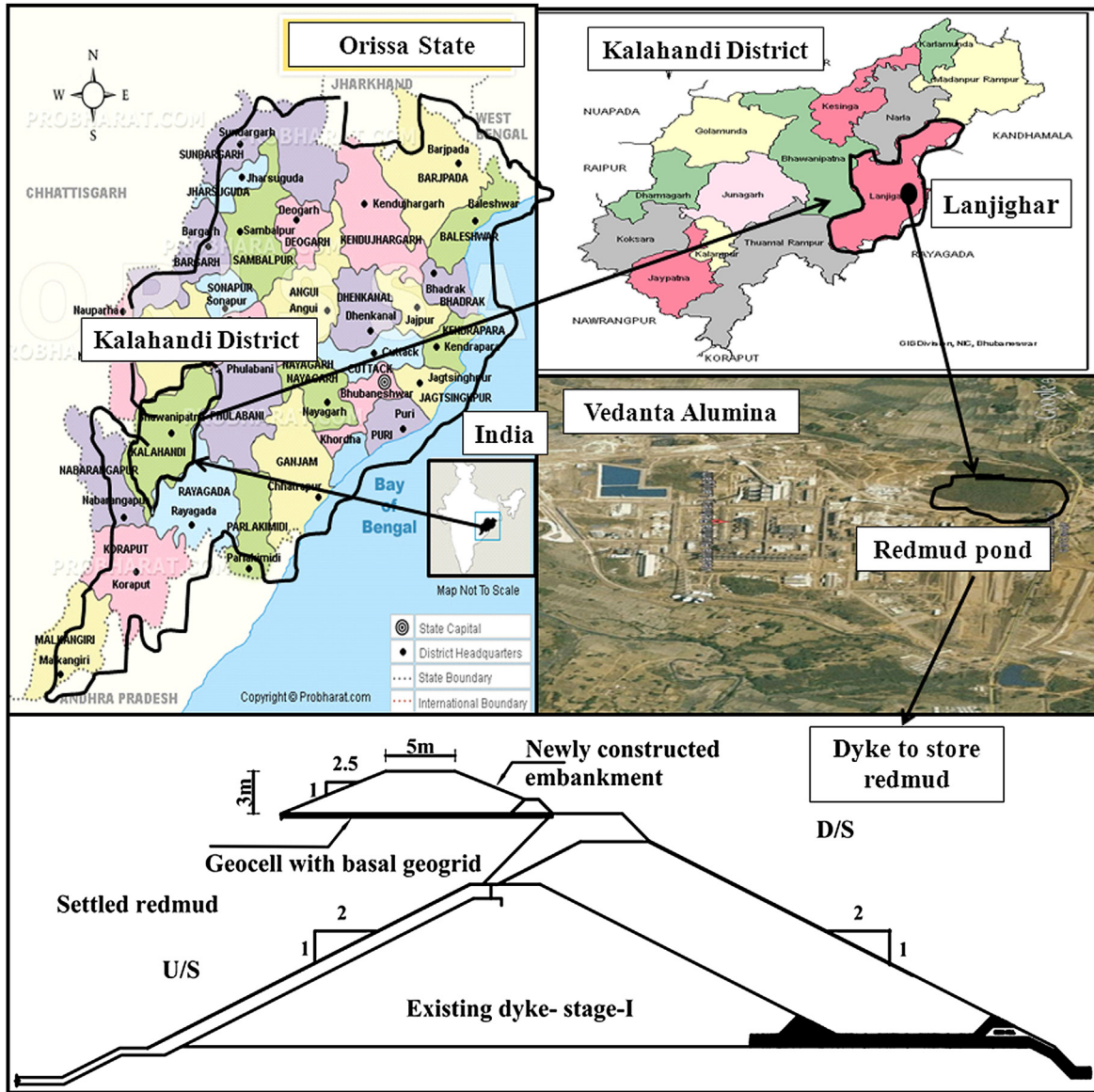


Fig. 1. Location, plan and typical cross section of the red mud dyke.

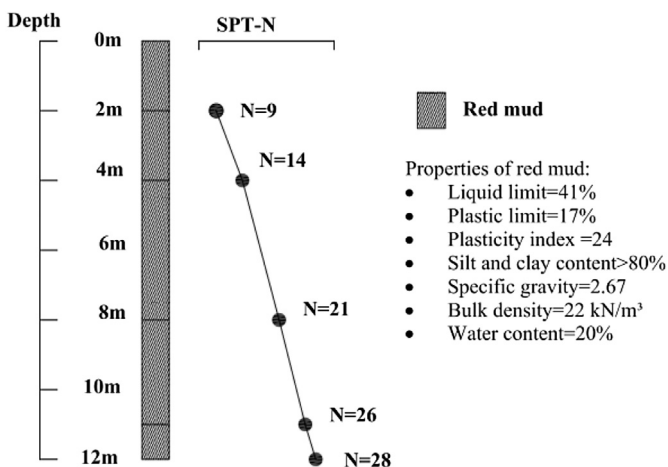


Fig. 2. Idealized soil profile of the area.

Undisturbed samples were collected at different locations of the test bed to determine the degree of saturation, unit weight, moisture content and the undrained shear strength of the soil mass. Properties of the clay bed are summarized in Table 2 and the same properties were maintained in all the three tests. Clay bed was freshly prepared from the dry soil for the every new test. Both geocell and geogrid were placed to the full width of the tank. The cell pockets were filled up with the clean sand using pluviation technique to achieve the relative density of 65%. A layer of geotextile was used as the separator between soft clay bed and the sand overlaying it. Upon filling the geocell with the sand, the fill surface was leveled.

4.4. Testing procedures

Footing was placed at the top of the bed at a predetermined alignment. A recess was made on the top surface of the footing and a ball bearing arrangement was placed into it. The ball bearing arrangement helps to apply the load at the center of the footing

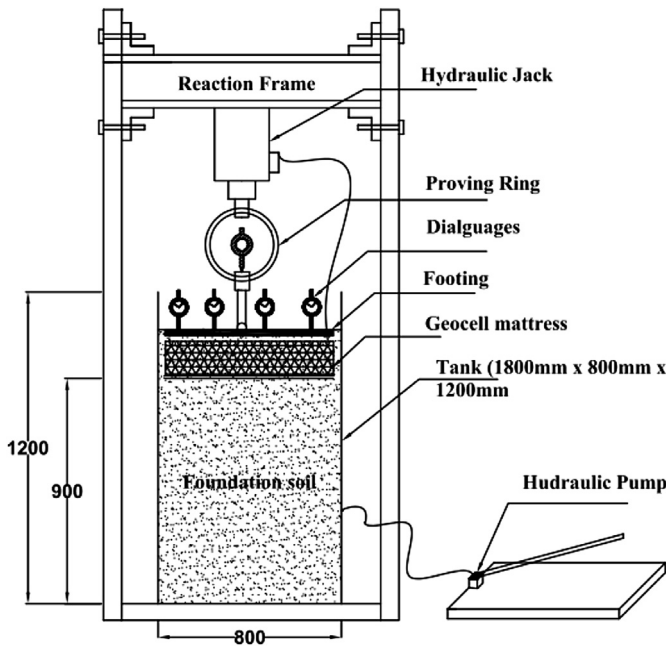


Fig. 3. Schematic view of the test setup.

Table 1
Properties of the geocell and geogrid.

Parameters	Quantity
Geocell	
Polymer	Polyethylene
Cell size(mm)	250 × 210
No. of cells/m ²	40
Cell depth (mm)	150
Strip thickness (mm)	1.53
Cell seam strength (N)	2150(±5%)
Density (g/cm ³)	0.95 (±1.5%)
Short term yield strength (kN/m)	20
Geogrid	
Polymer	Polypropylene
Aperture size (MD × XMD) mm	35 × 35
Ultimate tensile strength (kN/m)	20
Mass per unit area (g/m ²)	220
Shape of aperture opening	Square

clear failure was observed in the pressure settlement behavior even up to the large settlement of 45% of footing width. This can be attributed to the beam effect of the geocell mattress; due to its high bending and shear stiffness, geocell mattress can support the footing even after the failure of soil. The interconnected cells form a panel that acts like a large mat that spreads the applied load over the extended area, leading to an overall improvement in the performance of the foundation bed. Post-test exhumation of geocell has shown the deformation in the vertical and the horizontal ribs. The reason for this could be, the ribs of the geocells were subjected to circumferential stresses due to the shear failure of the soil mass within the geocell pockets. Provision of the additional geogrid layer at the base of the geocell mattress further increases the load carrying capacity of the foundation bed.

The increase in the bearing capacity due to the provision of the reinforcement can be measured through a non-dimensional parameter called bearing capacity improvement factor (I_f), which can be defined as the ratio of bearing capacity of reinforced bed to the bearing capacity of the unreinforced bed at the same settlement. Bearing capacity improvement factor is similar to the bearing capacity ratio as reported by Binquet and Lee (1975). Variations of I_f with the footing settlement for different tests are shown in Fig. 6. Bearing capacity improvement factors increase with the increase in the settlement. Maximum value of 4 was observed in case of the geocell reinforcement. $I_f = 4$ means, 4 times increment in the bearing capacity as compared to unreinforced clay bed. Due to the provision of the additional basal geogrid, bearing capacity improvement factor increases up to 5.

Fig. 7 quantifies the maximum surface deformation for the different combination of the reinforcements. In case of unreinforced bed, surface heaving was observed as indicated by the negative deformation in the Fig. 7. The surface heaving can be attributed to the local shear failure of the soil mass. Generally, local shear failure accompanies with the heaving of the surrounding soil. In the present case, distinct failure surface was not observed in the soil mass though there was a heaving. In case of the geocell

without any eccentricity. Through the precise measurements, the footing was placed exactly at the center of the test tank. The load applied was measured through the pre-calibrated proving ring placed between the footing and the hydraulic jack. Two dial gauges (D_1 and D_2) were placed on the either side of the center line of the footing to record the footing settlements. Another set of dial gauges (S_1 and S_2) was placed at the distance of $1.5B$ (B is the width of the footing) from the center line of the footing to measure the deformation underwent by the fill surface. The footing settlement (S) and the surface deformation (d) were normalized by footing width (B) to express them in non-dimensional form as S/B (%) and d/B (%). In all the plots, settlements are reported with the positive sign and the heave with the negative sign.

4.5. Results and discussion

Fig. 5 represents the bearing pressure – settlement responses for the different tests. Distinct failure was observed in case of the unreinforced case. However, in case of geocell reinforcement, no

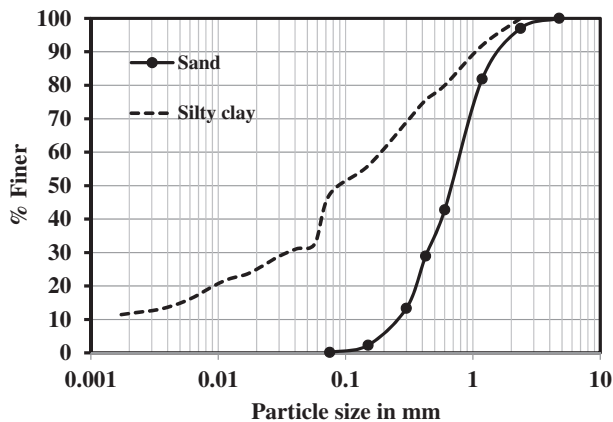


Fig. 4. Grain size distribution of the materials.

Table 2
Properties of the soft clay bed.

Parameters	Values
Moisture content (%)	20
Degree of saturation (%)	95
Bulk unit weight (kN/m ³)	20.2
Dry unit weight (kN/m ³)	14.81
Undrained shear strength (kPa)	10

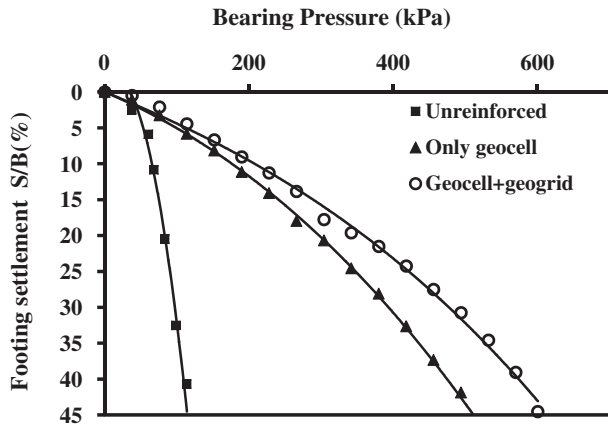


Fig. 5. Variation of bearing pressure with footing settlement.

reinforcement and the case of geocell with additional basal geogrid, no surface heaving was observed. The reason for this could be that the failure surfaces were completely arrested within the geocell pockets and hence preventing it from reaching the ground surface. The combination of geocell and geogrid shows lesser d/B (%) values as compared to the only geocell case at a given S/B (%). This is due to the membrane action of geogrid layer, which resists the downward deflection of the geocell mattress under footing load through mobilization of its strength (Dash et al., 2003).

4.5.1. Analytical studies

Zhao et al. (2009) reviewed the literature on geocell supported embankments and suggested that the geocell layer contributes to the strength through three main aspects: (a) lateral resistance effect, (b) vertical stress dispersion effect and (c) membrane effect. Further, Zhang et al. (2010) proposed simple bearing capacity calculation method for geocell supported embankment over the soft soil. This method considers only vertical stress dispersion mechanism and the membrane effect mechanism. Earlier, Koerner (1998) had provided the analytical solution to estimate the bearing capacity of the geocell reinforced foundation beds. The method proposed by Koerner considers only lateral resistance effect developed due to the interfacial friction between soil and cell wall. However, the present method considers all the three mechanisms proposed by Zhao et al. (2009) into the formulation.

This model is based on the hypothesis that the lateral resistance effect and the vertical stress dispersion effect mechanisms are originated by virtue of geocell while the membrane effect is contributed by basal geogrid. Experimental studies conducted by

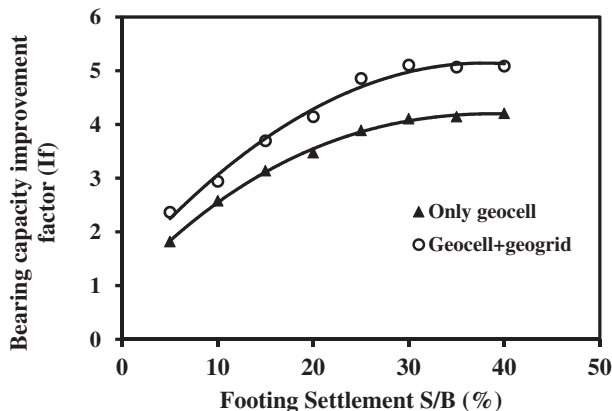


Fig. 6. Variation of bearing capacity improvement factors with footing settlement.

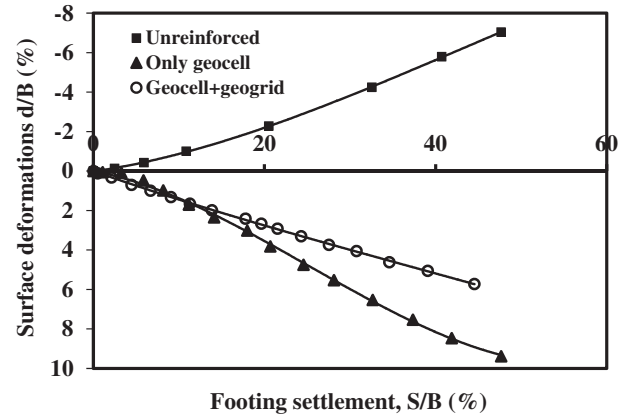


Fig. 7. Variation surface deformation with footing settlement.

the authors suggested that geogrid also contribute to the increase in the bearing capacity. It was also observed that geogrid undergoes considerable bending due to the application of footing load. Bending of the planar geogrid causes the mobilization of the tensile strength within the geogrid. The mobilized tensile strength in the geogrid will contribute to the membrane effect. However, geocell acts as a rigid slab; which undergoes uniform settlement without any significant bending (Dash et al., 2001a; Yang, 2010). Hence, membrane effect was not considered for only geocell case.

Increase in the load carrying capacity of the foundation bed is expressed in terms of applied pressure on the geocell mattress, tensile strength of the geogrid and the allowable limiting settlement. It is very relevant to express the increase in load carrying capacity in terms of pressure applied on the geocell mattress because of the mobilization of shear strength at the cell wall is directly related to applied pressure. The lateral resistance effect component (ΔP_l) is calculated using Koerner (1998) method:

$$\Delta P_l = 2\tau \tag{1}$$

where τ is the shear strength between the geocell wall and the infill soil and is given by,

$$\tau = P_r \tan^2(45 - \varphi/2) \tan \delta \tag{2}$$

where P_r is the applied vertical pressure on the geocell, φ is the friction angle of the soil used to fill the geocell pockets and δ is the angle of shearing resistance between the geocell wall and the soil contained within. Generally, value of δ is in the range of 15 to 20° between sand and HDPE (Koerner, 1998). In this particular case, $\delta = 18^\circ$ was considered.

The vertical stress dispersion mechanism is also called as wide slab mechanism. This mechanism was first observed by Binquet and

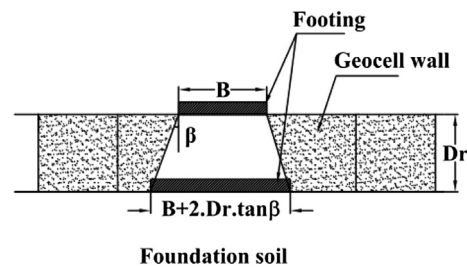


Fig. 8. Vertical stress dispersion mechanism in geocell reinforced beds.

Lee (1975). Schlosser et al (1983) extended this mechanism to the strip footing resting on the reinforced soil beds. Subsequently, many researchers have reported the wide slab mechanism in their studies (Huang and Tatsuoka, 1988, 1990; Takemura et al., 1992). In addition, the presence of a wide slab mechanism in the geocell reinforced foundation bed was justified by the findings of Dash et al. (2001a, b); Sitharam and Sireesh (2004, 2005) through 1-g model tests. They observed that the interconnected cells form a panel that acts like a large slab that spreads the applied load over an extended area leading to the overall improvement in the performance of the foundation soil. Fig. 8 is the schematic representation of the vertical stress dispersion mechanism in the geocell reinforced foundation beds. Footing of width B resting on the geocell reinforcement behaves as if the footing of width $B + \Delta B$ resting on soft soil at the depth of D_r , where D_r is the depth of the reinforcement and β is the load dispersion angle that varies between 30° to 45° . If P_r is the applied pressure on the footing with width B , then actual pressure transferred to the soil subgrade is less than P_r . Reduction in the pressure due to provision of geocell (ΔP_2) is obtained as,

$$\Delta P_2 = P_r \left(1 - \frac{B}{B + 2D_r \tan \beta} \right) \quad (3)$$

The membrane effect mechanism is contributed by the vertical component of the mobilized tensile strength of the planar reinforcement (Zhang et al., 2010). Hegde and Sitharam (2012) observed that provision of the basal geogrid will resist the downward movement of soil due to the footing penetration through experimental studies. Hence, membrane effect component was considered additionally in the formulation of the load carrying capacity of the foundation bed reinforced with combination of geocell and geogrid. The increase in the load carrying capacity due to the membrane effect (ΔP_3) is given by,

$$\Delta P_3 = \frac{2T \sin \alpha}{B} \quad (4)$$

where, T is the tensile strength of the basal geogrid material. $\sin \alpha$ is calculated as a function of settlement under the given load. The deformed shape of geogrid is generally parabolic in nature. However, if the footing dimension is very small compared to the geogrid dimension then it resembles the triangular shape. In the present case, geogrid dimension is 5.5 times larger than the footing dimension and hence the triangular shape was considered as indicated by dotted line in Fig. 9.

$$\sin \alpha = \frac{2S}{B_g} \quad (5)$$

where B_g is the width of the basal geogrid and S is the footing settlement measured at the surface. The increase in the load carrying capacity of the foundation bed reinforced with combination of geocell and geogrid is represented as:

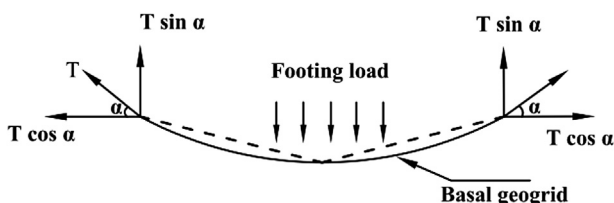


Fig. 9. Deformed basal geogrid contributing to membrane effect.

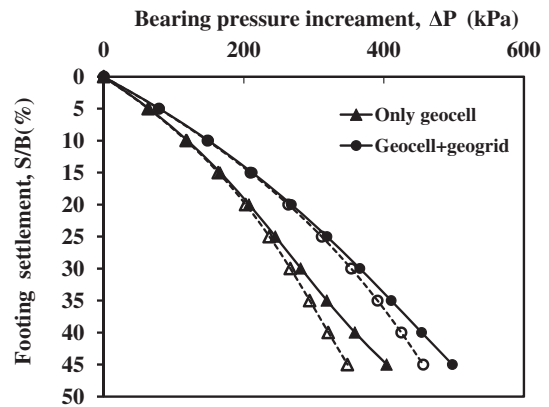


Fig. 10. Comparison of measured and calculated ΔP - S curve.

ΔP = lateral resistance effect + vertical stress dispersion effect + membrane effect

$$\Delta P = 2\tau + P_r \left(1 - \frac{B}{B + 2D_r \tan \beta} \right) + \frac{2T \sin \alpha}{B} \quad (6)$$

Fig. 10 represents the comparison of experimental and calculated ΔP - S curves for the two cases viz. only geocell reinforced case and combination of geocell and geogrid reinforced case. There exists a good match between measured and calculated ΔP values at the different settlements. Membrane effect was not considered in the evaluation of the increase in the load carrying capacity of the foundation bed reinforced with only geocell.

Experimental and analytical studies provided the vital clue about the use of combination of geocell and geogrid for the construction of the foundation for the embankment. Provision of the basal geogrid not only mobilizes the additional strength in the clay bed but also resists the downward movement of soil due to the footing penetration. Hence, it is always beneficial to use the combination of geocell and the geogrid.

5. Proposed foundation to support the embankment at the site

Based on the experimental and analytical studies, the geocell foundation system was proposed to support the embankment. A layer of geocell with height 0.15 m, pocket diameter 0.21 m and ultimate tensile strength 20 kN/m was recommended. A biaxial geogrid layer was also suggested at the base of the geocell mattress. The properties of the geocell and geogrid used in the experimental studies itself was suggested for the field construction also. In addition, it was suggested to extend the reinforcement by 1 m

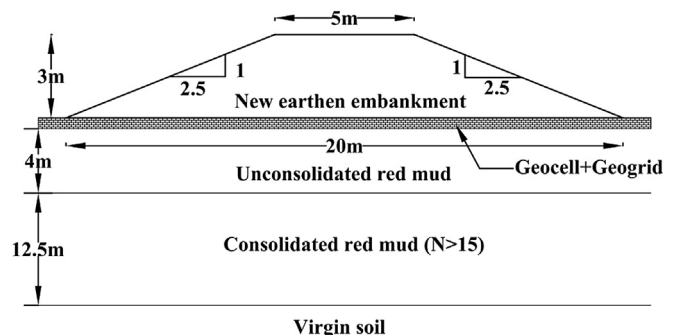


Fig. 11. Schematic representation of proposed foundation scheme.

beyond the base width of embankment on either side. Fig. 11 shows the schematic representation of the foundation scheme for the proposed embankment.

6. Construction sequence and methodology

A sand layer of thickness 200 mm was placed on the leveled ground for providing the drainage at the base. Above the sand layer, biaxial geogrid made up Polypropylene with aperture size 35 mm × 35 mm was placed. A minimum overlap of 300 mm was allowed between adjacent sheets of geogrids to avoid stitching. Then the geocells were unpacked and spread over the geogrid. The adjacent geocells were tied with special pins from the rolls. Once the geocell was placed for the entire base width, good quality granular soil (sand) was filled for the entire height of geocell. Front-end wheel loaders were used to fill the soil in the geocell.

7. Conclusions

Geocell foundation is cost effective and very simple to construct. Over 15,000 m² of embankment base was stabilized using geocell foundation in Lanjighar, Orissa. The foundation work was completed within 15 days using locally available labors and the equipment. The newly constructed embankment on the geocell foundation has already sustained two monsoon rains and continues to be functioning at its best condition. No cracks, seepage or settlements have been observed. Like Aluminum tailings (redmud), geocell foundations can also be used in various other mine tailings like zinc, copper etc. Geocell foundation can offer potential solution to storage problems faced by various mining industries across India. In addition, geocell reinforcement inevitably qualifies itself to support the road and rail embankments in the transportation sectors.

Experimental study suggested that the bearing capacity of the foundation bed increases by 4–5 times due to the provision of the combination of geocell and geogrid. The interconnected cells form a panel that acts like a large mat that transfers the imposed load to an extended area, leading to a better performance of the foundation bed. In addition, geocell reinforcement also reduces the footing settlement and the surface heaving. Hence, geocell foundation can be recommended to use as an alternative to the ground improvement techniques in soft soil. It is always beneficial to use the combination of the geocell and geogrid than using geocell alone. Provision of the basal geogrid not only mobilizes the additional strength in the clay bed but also resists the downward movement of soil due to the penetration of the footing.

A simple analytical model was proposed to estimate the increase in load carrying capacity of the clay bed reinforced with combination of geocell and geogrid. The solution was established by superimposing the three mechanisms viz. lateral resistance effect,

vertical stress dispersion effect and the membrane effect. By knowing the pressure applied on the geocell, tensile strength of the geogrid and the limiting settlement, the increment in the load carrying capacity can be calculated. The analytical model was validated with the experimental results and the results were found to be in good agreement with each other. However, further experimental studies are necessary with different shapes of the footing to calibrate the analytical model by incorporating the appropriate shape factors.

Notations

- B width of the footing (m)
- B_g width of basal geogrid (m)
- C_c coefficient of curvature (dimensionless)
- C_u coefficient of uniformity (dimensionless)
- d surface deformation (m)
- D_r height of the geocell (m)
- D_{10} effective particle size (mm)
- e_{max} maximum void ratio (dimensionless)
- e_{min} minimum void ratio (dimensionless)
- I_f bearing capacity improvement factor (dimensionless)
- ΔP total increase in load carrying capacity foundation soil due to the presence of the reinforcement (kPa)
- ΔP_1 increase in the load carrying capacity due to the lateral resistance effect (kPa)
- ΔP_2 increase in the load carrying capacity due to the vertical stress dispersion effect (kPa)
- ΔP_3 increase in the load carrying capacity due to the membrane effect (kPa)
- P_r pressure applied on the geocell reinforced soil (kPa)
- P_u pressure applied on the unreinforced soil (kPa)
- S footing settlement measured at the surface (m)
- T tensile strength of geogrid (kN/m)
- α horizontal angle of the tensional force T (degrees)
- β load dispersion angle (degrees)
- δ angle of shearing resistance between the geocell wall and soil (degrees)
- ϕ angle of internal friction of infill soil (degrees)
- τ shear strength between the geocell wall and the infill soil (kPa)

Abbreviations

- PVD Prefabricated Vertical Drains
- SPT Standard Penetration Test

Appendix A

Table 3
Comparison of analytical and experimental results: combination of geocell and geogrid.

$S/B(\%)$	$S(m)$	$P_r(kPa)$ experiment	ΔP_1 (kPa)	ΔP_2 (kPa)	ΔP_3 (kPa)	$\Delta P = \Delta P_1 + \Delta P_2 + \Delta P_3$ (kPa)	$P_u(kPa)$ experiment	$\Delta P = P_r - P_u$ (kPa) experiment
0	0.00	0.0	0.00	0.00	0.00	0.00	0.00	0.00
5	0.01	108.8	15.37	58.29	5.00	78.66	29.37	79.41
10	0.02	204.1	28.84	109.38	9.99	148.21	54.46	149.64
15	0.02	287.3	40.60	153.97	14.98	209.55	75.26	212.06
20	0.03	359.8	50.84	192.81	19.94	263.59	91.78	268.00
25	0.04	422.8	59.75	226.60	24.89	311.24	104.01	318.83
30	0.05	477.8	67.52	256.07	29.81	353.41	111.96	365.88
35	0.05	526.1	74.34	281.96	34.70	391.00	115.62	410.52
40	0.06	569.1	80.41	304.97	39.56	424.94	115.00	454.08
45	0.07	608.0	85.91	325.84	44.37	456.12	110.09	497.93

Table 4
Comparison of analytical and experimental results: only geocell.

S/B(%)	S(m)	P_r (kPa) experiment	ΔP_1 (kPa)	ΔP_2 (kPa)	$\Delta P = \Delta P_1 + \Delta P_2$ (kPa)	P_u (kPa) experiment	$\Delta P = P_r - P_u$ (kPa) experiment
0	0.00	0.0	0.00	0.00	0.00	0.00	0.00
5	0.01	94.2	13.31	50.48	63.79	29.37	64.82
10	0.02	174.1	24.59	93.27	117.87	54.46	119.59
15	0.02	241.7	34.16	129.55	163.71	75.26	166.48
20	0.03	299.4	42.31	160.47	202.78	91.78	207.66
25	0.04	349.3	49.36	187.20	236.56	104.01	245.31
30	0.05	393.6	55.61	210.91	266.53	111.96	281.61
35	0.05	434.4	61.37	232.77	294.14	115.62	318.73
40	0.06	473.8	66.95	253.93	320.89	115.00	358.84
45	0.07	514.2	72.66	275.57	348.23	110.09	404.12

Formulas

$$\Delta P_1 = 2P_r \tan^2(45 - \varphi/2) \tan \delta \quad (\varphi = 40^\circ, \delta = 18^\circ)$$

$$\Delta P_2 = P_r \left(1 - \frac{B}{B + 2 \cdot D_r \cdot \tan \beta} \right) \quad (B = 0.15\text{m}, D_r = 0, \beta = 30^\circ)$$

$$\Delta P_3 = \frac{2T \sin \alpha}{B} \quad (B = 0.15\text{m}, T = 20\text{kN/m})$$

References

- Abusharar, S.W., Zheng, J.J., Chen, B.G., Yin, J.H., 2009. A simplified method for analysis of a piled embankment reinforced with geosynthetics. *Geotext. Geomembr.* 27 (1), 39–52.
- Basudhar, P.K., Dixit, P.M., Gharpure, Deb, K., 2008. Finite element analysis of geotextile reinforced sand bed subjected to strip loading. *Geotext. Geomembr.* 26 (1), 91–99.
- Bergado, D.T., Teerawattanasuk, C., 2008. 2D and 3D numerical simulations of reinforced embankments on soft ground. *Geotext. Geomembr.* 26 (1), 39–55.
- Bia, Xiao-Hong., Huang, Xian-Zhi, Zhang, Wei, 2013. Bearing capacity of square footing supported by a geobelt-reinforced crushed stone cushion on soft soil. *Geotext. Geomembr.* 38, 37–42.
- Binquet, J., Lee, L.K., 1975. Bearing capacity tests on reinforced earth slabs. *J. Geotech. Eng. Div.* 101 (12), 1241–1255.
- Chen, Y.M., Cao, W.P., Chen, R.P., 2008. An experimental investigation of soil arching within basal reinforced and unreinforced piled embankments. *Geotext. Geomembr.* 26 (2), 164–174.
- Chu, J., Bo, M.W., Choa, V., 2006. Improvement of ultra-soft soil using prefabricated vertical drains. *Geotext. Geomembr.* 24 (6), 339–348.
- Cowland, J.W., Wong, S.C.K., 1993. Performance of a road embankment on soft clay supported on a geocell mattress foundation. *Geotext. Geomembr.* 12, 687–705.
- Dash, S.K., Krishnaswamy, N.R., Rajagopal, K., 2001a. Bearing capacity of strip footings supported on geocell reinforced sand. *Geotext. Geomembr.* 19, 235–256.
- Dash, S.K., Krishnaswamy, N.R., Rajagopal, K., 2001b. Strip footing on geocell reinforced sand beds with additional planar reinforcement. *Geotext. Geomembr.* 19, 529–538.
- Dash, S.K., Sireesh, S., Sitharam, T.G., 2003. Model studies on circular footing supported on geocell reinforced sand underlain by soft clay. *Geotext. Geomembr.* 21 (4), 197–219.
- Demir, Ahmet., Laman, Mustafa., Yildiz, Abdulazim, Ornek, Murat., 2013. Large scale field tests on geogrid reinforced granular fill underlain by soft clay. *Geotext. Geomembr.* 38, 1–15.
- Fan, C.C., Hsieh, C.C., 2011. The mechanical behavior and design concerns for a hybrid reinforced earth embankment built in limited width adjacent to a slope. *Comp. Geotech.* 38 (2), 233–247.
- Ghazavi, M., Lavasan, A.A., 2008. Interference effect of shallow foundations constructed on sand reinforced with geosynthetics. *Geotext. Geomembr.* 26 (5), 404–415.
- Hegde, A., Sitharam, T.G., 2012. Performance of shallow footing on geocell reinforced sand beds using 1-g model tests. In: *Proceedings of Geosynthetics Asia 2012*, Bangkok, Thailand, pp. 757–762.
- Huang, J., Han, J., 2009. 3D coupled mechanical and hydraulic modeling of a geosynthetic reinforced deep mixed column supported embankment. *Geotext. Geomembr.* 27 (4), 272–280.
- Huang, C.C., Tatsuoka, E., 1988. Prediction of bearing capacity in level sandy ground reinforced with strip reinforcement. In: *Proceedings International Geotechnical Symposium on Theory and Practice of Earth Reinforcement*. Balkema, Fukuoka, Kyushu, Japan, pp. 191–196.
- Huang, C.C., Tatsuoka, E., 1990. Bearing capacity of reinforced horizontal sandy ground. *Geotext. Geomembr.* 9, 51–82.
- Indraratna, B., Nimbalkar, S., Christie, D., Rujikiatkamjorn, C., Vinod, J., 2010. Field assessment of the performance of a ballasted rail track with and without geosynthetics. *ASCE J. Geotech. Geoenviron. Eng.* 136, 907–917.
- Indraratna, B., Rujikiatkamjorn, C., Balasubramaniam, A.S., McIntosh, G., 2012. Soft ground improvement via vertical drains and vacuum assisted preloading. *Geotext. Geomembr.* 30, 16–23.
- Jenner, C.G., Bush, D.I., Bassett, R.H., 1988. The use of slip line fields to assess the improvement in bearing capacity of soft ground given by a cellular foundation mattress installed at the base of an embankment. In: *Proceedings of International Geotechnical Symposium on Theory and Practice of Earth Reinforcement*. Balkema, Rotterdam, pp. 209–214.
- Jones, B.M., Plaut, R.H., Filz, G.M., 2010. Analysis of geosynthetic reinforcement in pile supported embankment. Part I: 3D plate model. *Geosynth. Int.* 17 (2), 59–67.
- Karstunen, M., Yin, Z.Y., 2010. Modeling time dependent behavior of Murro test embankment. *Geotechnique* 60 (10), 735–749.
- Karunaratne, G.P., 2011. Prefabricated and electrical vertical drains for consolidation of soft clay. *Geotext. Geomembr.* 29 (4), 391–401.
- Koerner, R.M., 1998. *Designing with Geosynthetics*. Prentice Hall, New Jersey.
- Krishnaswamy, N.R., Rajagopal, K., Madhavi Latha, G., 2000. Model studies on geocell supported embankments constructed over a soft clay foundation. *Geotech. Test. J.*, ASTM, 45–54.
- Lambert, S., Nicot, F., Gotteland, P., 2011. Uniaxial compressive behavior of scrapped tire and sand filled wire netted geocell with a geotextile envelope. *Geotext. Geomembr.* 29, 483–490.
- Leshchinsky, Ben., Ling, Hoe I., 2013. Numerical modeling of behavior of railway ballasted structure with geocell confinement. *Geotext. Geomembr.* 36, 33–43.
- Li, A.L., Rowe, R.K., 2008. Effects of viscous behavior of geosynthetic reinforcement and foundation soils on the performance of reinforced embankments. *Geotext. Geomembr.* 26, 317–334.
- Lorenzo, G.A., Bergado, D.T., Bunthai, W., Homdee, D., Phothiraksanon, P., 2004. Innovations and performances of PVD and dual function geosynthetic applications. *Geotext. Geomembr.* 22, 75–99.
- Madhavi Latha, G., 2000. *Investigations on the Behavior of Geocell Supported Embankments*. Ph.D. thesis. Indian Institute of Technology, Madras, India.
- Madhavi Latha, G., Somwanshi, A., 2009. Effect of reinforcement form on the bearing capacity of square footing on sand. *Geotext. Geomembr.* 27, 409–422.
- Madhavi Latha, G., Rajagopal, K., Krishnaswamy, N.R., 2006. Experimental and theoretical investigations on geocell supported embankments. *Int. J. Geomech.* 6 (1), 30–35.
- Magnani, H.O., Almeida, M.S.S., Ehrlich, M., 2009. Behavior of two test embankments on soft clay. *Geosynth. Int.* 16 (3), 127–138.
- Mehdipour, Iman., Ghazavi, Mahmoud, Moayed, R.Z., 2013. Numerical study on stability analysis of geocell reinforced slopes by considering the bending effect. *Geotext. Geomembr.* 37, 23–34.
- Moghaddas Tafreshi, S.N., Dawson, A.R., 2010. Behavior of footings on reinforced sand subjected to repeated loading comparing use of 3D and planar geotextile. *Geotext. Geomembr.* 28, 434–447.
- Moghaddas Tafreshi, S.N., Dawson, A.R., 2012. A comparison of static and cyclic loading responses of foundations on geocell reinforced sand. *Geotext. Geomembr.* 32 (5), 55–68.
- Pokharel, S.K., Han, J., Leshchinsky, D., Parsons, R.L., Halahmi, I., 2010. Investigation of factors influencing behavior of single geocell reinforced bases under static loading. *Geotext. Geomembr.* 28 (6), 570–578.
- Rowe, R.K., Taechakumthorn, C., 2008. Combined effect of PVDs and reinforcement on embankments over rate sensitive soils. *Geotext. Geomembr.* 26 (3), 239–249.
- Rowe, R.K., Taechakumthorn, C., 2011. Design of reinforced embankments on soft clay deposits considering the viscosity of both foundation and reinforcement. *Geotext. Geomembr.* 29, 448–461.
- Saowapakpipoon, J., Bergado, D.T., Youwai, S., Chai, J.C., Wanthong, P., Voottipruex, P., 2010. Measured and predicted performance of prefabricated

- vertical drains (PVDs) with and without vacuum preloading. *Geotext. Geomembr.* 28 (1), 1–11.
- Schlösser, E., Jacobsen, H.M., Juran, I., 1983. Soil reinforcement. General Report. In: 8th European Conference on Soil Mechanics and Foundation Engineering. Balkema, Helsinki, pp. 83–103.
- Sharma, J.S., Bolton, M.D., 2001. Centrifugal and numerical modeling of reinforced embankments on soft clay installed with wick drains. *Geotext. Geomembr.* 19, 23–44.
- Sinha, A.K., Havanagi, V.G., Mathur, S., 2009. An approach to shorten the construction period of high embankment on soft soil improved with PVD. *Geotext. Geomembr.* 27 (6), 488–492.
- Sireesh, S., Sitharam, T.G., Dash, S.K., 2009. Bearing capacity of circular footing on geocell sand mattress overlying clay bed with void. *Geotext. Geomembr.* 27 (2), 89–98.
- Sitharam, T.G., Sireesh, S., 2004. Model studies of embedded circular footing on geogrid reinforced sand beds. *Ground Improv.* 8 (2), 69–75.
- Sitharam, T.G., Sireesh, S., 2005. Behavior of embedded footings supported on geocell reinforced foundation beds. *Geotech. Test. J.* 28 (5), 452–463.
- Subaida, E.A., Chandrakaran, S., Sankar, N., 2009. Laboratory performance of unpaved roads reinforced with woven coir geotextiles. *Geotext. Geomembr.* 27 (3), 204–210.
- Takemura, J., Okamura, M., Suesmasa, N., Kimura, T., 1992. Bearing capacity and deformations of sand reinforced with geogrids. In: *Proceedings of Earth Reinforcement Practice*. Balkema, Fukuoka, Kyushu, Japan, pp. 695–700.
- Tavakoli Mehrjardi, Gh., Moghaddas Tafreshi, S.N., Dawson, A.R., 2012. Combined use of geocell reinforcement and rubber soil mixtures to improve performance of buried pipes. *Geotext. Geomembr.* 34, 116–130.
- Thakur, J.K., Han, Jie., Pokharel, S.K., Parsons, R.L., 2012. Performance of geocell-reinforced recycled asphalt pavement (RAP) bases over weak subgrade under cyclic plate loading. *Geotext. Geomembr.* 35, 14–24.
- Wang, L., Zhang, G., Zhang, J.M., 2011. Centrifuge model tests of geotextile reinforced soil embankments during an earthquake. *Geotext. Geomembr.* 29 (3), 222–232.
- Yang, X., 2010. Numerical Analysis of Geocell Reinforced Granular Soils under Static and Repeated Loads. Ph.D. thesis. University of Kansas, USA.
- Yang, X., Han, J., Pokharel, S.K., Manandhar, C., Parsons, R.L., Leshchinsky, D., Halahmi, I., 2012. Accelerated pavement testing of unpaved roads with geocell reinforced sand bases. *Geotext. Geomembr.* 32, 95–103.
- Zhang, L., Zhao, M., Shi, C., Zhao, H., 2010. Bearing capacity of geocell reinforcement in embankment engineering. *Geotext. Geomembr.* 28, 475–482.
- Zhao, M.H., Zhang, L., Zou, X.J., Zhao, H., 2009. Research progress in two direction composite foundation formed by geocell reinforced mattress and gravel piles. *Chinese J. Highw. Trans.* 22 (1), 1–10.
- Zheng, J.J., Chen, B.G., Lu, Y.E., Abusharar, S.W., Yin, J.H., 2009. The performance of an embankment on soft ground reinforced with geosynthetics and pile walls. *Geosynth. Int.* 16 (3), 173–182.
- Zhou, H., Wen, X., 2008. Model studies on geogrid or geocell reinforced sand cushion on soft soil. *Geotext. Geomembr.* 26, 231–238.